MOF-Supported Heterogeneous Catalysts for Hydroformylation Reactions: A Minireview

P. Samanta, J. Canivet

MOF-Supported Heterogeneous Catalysts for Hydroformylation Reactions: A Minireview

Partha Samanta,* [a] and Jerome Canivet*[b]

[a] Dr. Partha Samanta
Institut Català de Nanociència i Nanotecnologia (ICN2)
UAB Campus, Bellaterra (Barcelona)
08193, Spain
E-mail: partha.samanta@icn2.cat

[b] Dr. Jerome Canivet
Univ. Lyon, Université Claude Bernard Lyon 1, CNRS, IRCELYON - UMR 5256,
2 Av. Albert Einstein, 69626 Villeurbanne Cedex, France.
E-mail: jerome.canivet@ircelyon.univ-lyon1.fr

Abstract: Transition metal-catalyzed hydroformylation reaction of olefins is one of the most important transformations in the perspective of both industrial applications and academic research. This synthetic process provides a straightforward and easy way for the transformations of inexpensive feedstock (mostly different alkene molecules) to valuable aldehyde compounds, which are considered as major building blocks for several essential chemical products. Inspired and motivated by the tremendous success of homogeneous catalysis for hydroformylation reactions, paramount interests have been raised for the design and development of active heterogeneous catalysts owning advantages from both molecular and material sciences. Crystalline metal-organic frameworks (MOFs) as solid support to immobilize active catalysts for the hydroformylation reaction have shown appealing promises as heterogeneous catalysts. This review sketches out a decade of developments of MOF-based heterogeneous catalysts for the hydroformylation of olefins while discussing both advantages and limitations for their implementation beyond the lab scale.

1. Introduction

In 1938 hydroformylation reaction was discovered accidentally by Otto Roelen, while investigating the Fischer-Tropsch reaction.[1,2] Also known as “Oxo process”, this reaction adds carbon monoxide (CO) and hydrogen to the alkene molecules to form corresponding aldehydes in a one step process with 100% atom efficiency.[3] Moreover, in recent days hydroformylation reaction is considered as one of the most important synthetic tools for the synthesis of C-C bond directly leading to the value-added aldehydes and their derivatives such as alcohols, acids, etc. Such products, obtained from hydroformylation reaction, are very much essential for the production of detergents or surfactants, polymer plasticizers, industrial solvents, etc.[4,5] As a consequence of high demand, in recent years it has been estimated that more than 12 million tons of oxo-products are being produced industrially every year.[3] On the other hand, hydroformylation reaction of alkenes can lead to the formation of mixture of isomeric products, i.e., *n*-alddehydes (linear) and *i*-aldehydes (branched), except in the case of ethylene, where only one type of aldehyde product is expected (*n*-alddehyde) (Scheme 1). Moreover, due to the possibility in the isomerization of the olefin bonds of respective alkenes, many different types of branch aldehydes can be formed from a single olefin moiety. So, not only the conversion of respective alkenes, but also the regioselectivity of products is very important for the design of the catalysts in this regard. Till date, mostly rhodium (Rh) and cobalt (Co) have been used for this purpose as catalysts in both academic and industrial research. However, there are many other metals of interest for this reaction, and the order for the activity and regioselectivity is as follows, Rh >> Co > Ir > Ru > Pd > Mn > Fe > Ni >> Re.[3] Again, hydroformylation reaction is considered as the largest industrially relevant process runs by homogeneous catalysts. Initially, cobalt based homogeneous catalysts were used to synthesize aldehydes from alkenes. But, in 1965 Wilkinson demonstrated that rhodium based catalyst ($RhCl(PPh_3)_3$ type) can perform more efficiently under milder conditions than that of cobalt catalysts with higher conversion of olefins as well as regioselectivity or stereoselectivity of the respective products.[2] Many different types of linkers have been used for the preparation of Rh-based homogeneous catalysts to improve the efficiency and regioselectivity of the reaction. Although the homogeneous rhodium catalysts have found huge applicability in the hydroformylation reaction, there are still some issues to address in order to gain efficiency.[2,6–8] Often the phosphine linkers of the homogeneous catalysts leach during the catalytic process, which leads to the deactivation of the active catalysts. Then, more phosphine linkers are added during the process, which is a very essential step to continue the catalysis. Also, the separation of rhodium catalysts contaminants from the respective aldehyde products after the completion of reaction is also a very tedious and energy consuming process. In this context, heterogenized molecular catalysts represent appealing opportunities to tackle the aforementioned issues. Immobilization of homogeneous catalysts (or metal-salt precursors) on solid supports allows for an easy separation of the heterogeneous catalysts after the catalysis process. On the other hand, such supports made with phosphine linkers can act as “ligand reservoir”. Consequently, this would minimize the deactivation of the catalysts, and the catalytic process can be continued for several runs without addition of fresh organic linker. Many types of solid supports have been reported for the

design of heterogeneous catalysts for hydroformylation reactions, which include zeolites, silica, porous organic polymers (POPs), metal-organic frameworks (MOFs), etc.[2,3,5,9–22] The last decade has seen the emergence and evolution of MOFs based heterogeneous catalysts for the hydroformylation of olefins.

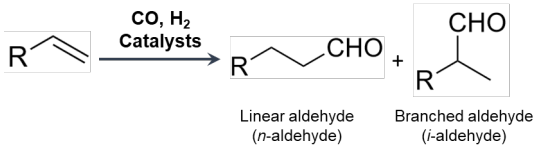

Scheme 1. a) Schematic representation of hydroformylation reactions of alkenes.

Owing to its high crystallinity, high surface area, tuneable pore surface, MOFs based heterogeneous catalysts have emerged as one of the suitable and appealing class of materials candidates.[10,23,24–37] Systematic development of heterogeneous catalysts based on MOFs is being described in this review. This review demonstrates the evolution of rhodium or cobalt based MOF-catalysts for the hydroformylation of olefins, from metal nanoparticles infiltrated catalysts to well defined site-isolated molecular catalysts immobilized materials.

Dr. Partha Samanta completed his B.Sc. degree in 2011 and M.Sc. degree in 2013 from the University of Calcutta and IIT Kharagpur, respectively. Then, he joined the research group of Dr. Sujit K. Ghosh at IISER Pune to pursue his doctoral studies. In 2019, he obtained a PhD degree and then he joined IRCELYON as postdoctoral fellow with Dr. Jerome Canivet, where he worked on heterogeneous catalysts for important organic transformations. And currently, he is working with Dr. Daniel Maspoch at ICN2 (Barcelona, Spain) as postdoctoral researcher, and his research interest is focused on the Clip-off chemistry of reticular materials.

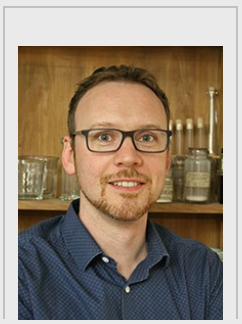

Dr. Jérôme Canivet was appointed CNRS researcher at the IRCELYON in 2010. He works at developing innovative catalytic processes for sustainable fine chemicals and energy. His research topics range from C-C coupling to asymmetry, photocatalysis and green fuels. In 2018, he received the Young Investigator Award from the Catalysis Division of the French Chemical Society for creating trends reducing the gap between homogeneous and heterogeneous catalysis. He further aims at exploiting the confinement of molecular catalytic systems into porous structures for the improvement of their catalytic activity and selectivity, and he is coordinating cooperative projects on this topic.

2. Heterogenized MOF-based catalysts for hydroformylation of alkenes

In recent years, several MOFs based catalysts have been reported for the alkene hydroformylation reaction after immobilizing rhodium or cobalt precursors inside their porous networks. In early reports, highly distributed rhodium nanoparticles inside MOFs showed promising results as heterogeneous catalysts for various hydroformylation reactions. More recently, the heterogenization of site-isolated molecular catalysts inside porous networks of MOFs has emerged to synthesize heterogeneous catalysts with well-defined isolated active sites for olefin hydroformylations.

2.1 Ligand-less rhodium species within MOFs

Herein are reported MOF-based catalysts containing rhodium species without organic ligands, like phosphines. These examples can refer to single-atom catalysts, based on their preparation and nature, which imply no or weak influence of the first coordination sphere of immobilized metal atom.[38–40]

In 2012, Vu *et al.* demonstrated the use of MOF support for rhodium based heterogeneous catalysts for the hydroformylation of olefins.[41] In this case, MOF-5, synthesized from $Zn(NO_3)_2$ and terephthalic acid (H_2BDC), was used as a solid support for the immobilization of Rh(I)-precursor to prepare the catalyst Rh/MOF-5. Powder X-ray diffraction (PXRD) pattern of the Rh/MOF-5 catalyst was found to be in a good match with that of the as-synthesized MOF-5. Also, from transmission electron microscopy (TEM) images no particles of rhodium were observed. This led to the conclusion that highly dispersed rhodium based catalyst maintained the structural integrity as MOF-5. The catalytic efficiency of the catalyst was tested with linear alkene, such as n-hex-1-ene, n-oct-1-ene, n-dec-1-ene, and n-dodec-1-ene, and some branched olefins, such as 3,3-dimethyl-1-butene, 4,4-dimethyl-1-pentene, and 2,4,4-trimethyl-1-pentene. Some bulky olefins like cyclohexene and cyclooctene were also used to understand the efficiency of Rh/MOF-5. In toluene at 100 °C and under 50 bars pressure of the syngas, a total olefins conversion of 99%, 90%, and 67% were observed after 5 hours for n-hexene-1, n-decene-1, and n-dodecene-1, respectively; while yields of aldehydes were found to be 45%, 27%, and 19%, respectively. The difference in the total conversion of alkenes and yields of aldehydes were attributed to isomerization of n-alkenes to their corresponding *i*-alkenes (branched). When the catalysis process was continued until 21 hours, an improved yield of aldehyde was obtained in all cases, since *i*-alkenes were also converted into i-aldehydes with higher reaction duration. However, the *n/i*-aldehydes selectivity decreased with higher reaction time, as production of *i*-aldehydes increased with time. Furthermore, to examine the influence of the texture of MOF-5, authors prepared two more catalysts with nano-sized MOF-5 having more intergrown and slightly smaller particles, and another with larger well-crystallized MOF-5 crystals. The BET (Brunauer-Emmett-Teller) surface areas of these MOFs were found to be 2337, 576 and 1200 $m^2 g^{-1}$ for previously discussed MOF-5 (agglomerated particles), nano-sized MOF-5 with smallest particle size (intergrown particles) and larger well-crystallized MOF-5 (microcrystalline), respectively. Hydroformylation of n-1-hexene showed a better efficiency in conversion of olefin and yields of aldehydes with

larger well-crystallized MOF-5 based catalyst. However, *n/i*-aldehydes selectivity was decreased as compared to the former Rh/MOF-5 with agglomerated particles. While both nano-sized MOF-5 based demonstrated almost similar activity, the *n/i*-aldehydes selectivity was found to be improved for the nano-sized intergrown MOF-5. Larger and well-crystallized MOF-5 provided better accessibility of olefin molecules to the active catalytic sites, resulting in better efficiency towards yields of aldehydes. While because of the diffusion limitation in case of both nano-sized MOF-5 by lattice defects, catenation or intergrowth, accessibility of alkenes to the active sites is comparatively lower, especially for *i*-alkenes.

In 2013, the same group reported another rhodium based heterogeneous catalyst with an amine ($-NH_2$) functionalized iso-structural MOF to MOF-5, namely, IRMOF-3.[42] This IRMOF-3 was made of Zn(II) and 2-aminoterephthalic acid. However, after rhodium loading, the BET surface area of the Rh@IRMOF-3 was reduced from 2450 $m^2\ g^{-1}$ to 1874 $m^2\ g^{-1}$, attributed to both the incorporation of rhodium and partial damages to MOF crystals. In the XPS analysis of Rh@IRMOF-3, spectra corresponding to rhodium species were not observed due to its very low loading of 0.11 wt%. However, noticeable impact was observed in the appearance and location of XPS signals corresponding to Zn_{2p}, O_{1s}, and C_{1s}, while N_{1s} signal was found to be splitted into two components. Based on this observation, the authors confirmed the presence of rhodium species inside the pores of the MOF, more specifically, probably near the metal oxide sites. Moreover, for the hydroformylation of olefins, the authors used the same conditions as in their earlier report. In the catalytic process, total conversions of 30–45% for n-hexene-1, n-decene-1, and n-dodecene-1 were obtained after 1 hour, while for n-octene-1 only 5% was obtained. The low activity in case of n-octene-1 was explained as the limited access of it to the active sites. Again, the conversions for bulky alkene (cyclohexene) or sterically crowded alkene (2,2,4-trimethylpentene) were even slower. Recyclability test of the catalyst showed a decrease in the catalytic activity, but the selectivity (*n/i*-aldehydes) was maintained.

In 2013, the same group reported another highly porous MIL-101(Cr) (MIL: Materials of Institute Lavoisier) supported Rh-catalyst for hydroformylation of alkenes, where [(acetylacetonato)(1,5-cyclooctadiene)]Rh(I) was used as the metal precursor.[43] The structural integrity of the catalyst was found to be maintained as MIL-101(Cr) as confirmed by powder X-ray diffraction. TEM images showed the well dispersion of rhodium without forming any aggregates within the MOF. This observation was further supported by the small-angle X-ray scattering (SAXS) experiment, where no additional scattering corresponding to the small nano-sized rhodium was observed from catalyst. Interestingly, a significant amount of shift in the X-ray photoelectron spectroscopy was observed for both chromium (Cr) and oxygen (O) after the incorporation of Rh, but minor change was reported for the carbon. However, Rh was again not detected in the XPS study, due to its low loading wihtin the material. It was speculated that acetylacetonato linkers of the Rh-precursor were replaced by the oxygen atoms located at the $Cr_3O(OH)$ node to form Rh-O bonds. This conclusion was further supported by the infrared (IR) spectra of the MIL-101 and Rh@MIL-101. Again, all chromium sites in the MOF were uniformly distributed and well separated by the organic linkers, which resulted in the high dispersion of the Rh-sites in the catalyst. Then, catalytic activity of Rh@MIL-101 was tested several linear with different chain length, namely, n-hex-1-ene, n-oct-1-ene, n-dec-1-ene, n-dodec-1-ene, and n-hexadec-1-ene along with some other bulky olefins. The catalysis was carried in toluene with a 70,000/1 olefin/catalyst ratio (based on Rh) at 100 °C. After 1 hour of reaction, the conversion of the respective alkenes was found to be proportional to their chain length with the exception of n-oct-1-ene, and the order of reactivity was n-hex-1-ene > n-dec-1-ene > n-dodec-1-ene > n-oct-1-ene >> n-hexadec-1-ene. Moreover, 20-30% aldehyde selectivity was obtained with Rh@MIL-101 and the remaining 70-80% of products was ascribed as the isomerized internal alkene derivatives. And these internal alkenes (olefin moieties were more sterically hindered than n-alk-1-ene) were barely transformed to the corresponding aldehydes due to their lack of accessibility of active Rh-sites located in the supertetrahedra (ST) with smaller windows sizes inside MOF. On the other hand, during the first 1-3 hours of reaction,linear to branched aldehydes ratio was 2.5-3.0, which then diminished with increasing time as a result of the Aldol condensation as a side reaction promoted by Lewis acid sites of MIL-101.

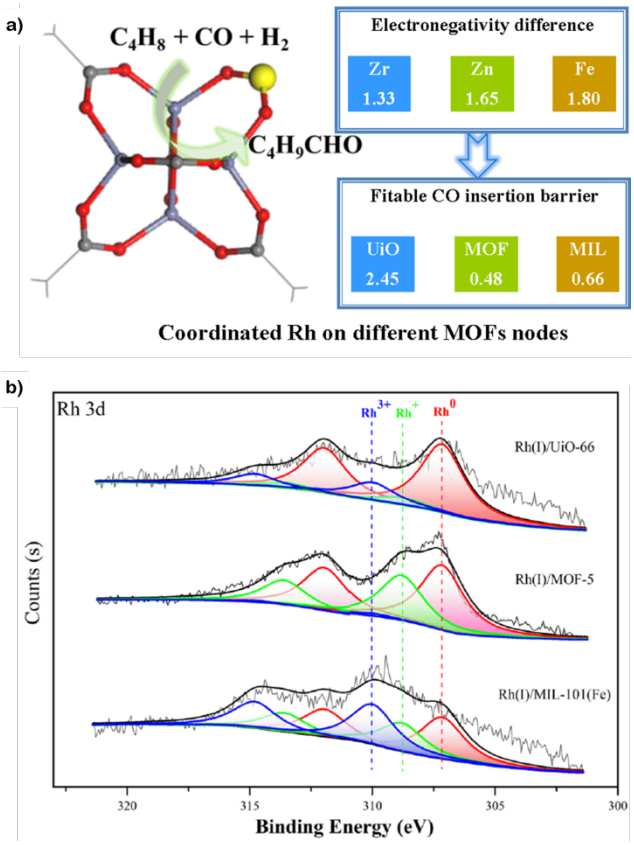

Figure 1. a) The effect of metal nodes of respective MOFs on the active Rh catalyst for n-butene hydroformylation reaction (the rhodium atom is depicted as yellow sphere); b) XPS spectra of Rh 3d for Rh(I)/UiO-66, Rh(I)/MOF-5 and Rh(I)/MIL-101(Fe) catalysts. Reproduced with permission from ref. 44. Copyright 2022, Elsevier.

In a recent study, Chen and co-workers demonstrated the usefulness of unsaturated secondary building units (SBUs) to obtain highly dispersed spatially separated Rh-sites inside the

MOFs.[44] Three different MOFs with different SBUs were employed, namely, UiO-66, MOF-5, and MIL-101 (Fe), respectively. The electronic effect of the respective SBUs environment near the active Rh-site was also evaluated. Thermogravimetric analysis (TGA) of aforementioned MOFs was used to calculate the number of missing linkers in the SBUs and revealed that for Zr_6 (UiO-66), Zn_4 (MOF-5) and Fe_3 (MIL-101 (Fe)) nodes this number was 2.1, 1.2, and 1.7, respectively. After the infiltration of Rh(I), Rh(I)/UiO-66, Rh(I)/MOF-5 and Rh(I)/MIL-101(Fe) MOFs based catalysts showed similar diffraction patterns in PXRD as their respective as-synthesized MOFs, which indicated that the structural integrity was maintained during the rhodium immobilization. Again, a decrease in the surface area of all catalysts as compared to the as-synthesized MOFs depicted the successful impregnation of rhodium. No rhodium nanoparticles were observed from TEM images. Furthermore, XPS studies of all MOF-catalysts revealed the presence of Rh^0 (307.6 eV), Rh^+ (308.8 eV), and Rh^{3+} (310.0 eV) (Fig. 1b). From these results, the valence states of Rh were found to be 0.27, 0.42 and 0.62 for Rh(I)/UiO-66, Rh(I)/MOF-5 and Rh(I)/MIL-101, respectively. This finding correlated with the electronegativity of respective node as follows Fe (1.80) > Zn (1.65) > Zr (1.33), where, increasing electronegativity led to transfer of more electron from rhodium to the respective node metals. Combining the XPS and DRIFT studies, the authors concluded that among all MOF supports MOF-5 based catalyst (Rh(I)/MOF-5) being constructed from Zn, could efficiently stabilize the CO molecules involved in the hydroformylation process leading to the improvement of the aldehyde selectivity (Fig. 1a). The catalytic activity of Rh(I)/UiO-66, Rh(I)/MOF-5 and Rh(I)/MIL-101(Fe) was evaluated with hydroformylation reaction of 1-butene at 100 °C under 20 bars of syngas (1:1 $CO:H_2$) for 4 hours. As it was anticipated, the highest catalytic activity was obtained with Rh(I)/MOF-5 catalyst, where conversion of alkene and selectivity in pentanal were found to be 96.4% and 85.8%, respectively. When the temperature was increased to 120 °C, both conversion of alkene and aldehyde selectivity increased. Additionally, with increment in the pressure of syngas the aldehyde selectivity was also increased along with the *n/i*-aldehyde selectivity. It is noteworthy to mention that authors also studied the catalytic activity with rhodium infiltrated corresponding metal oxide ($Rh(I)/MO_x$) as catalysts ($Rh(I)/ZrO_2$, Rh(I)/ZnO and $Rh(I)/Fe_2O_3$). Catalytic performance of Rh(I)/MOF-5 was found to be higher as compared to that of Rh(I)/ZnO. This result was explained in the light of dispersion of active rhodium catalysts on the respective solid supports; as rhodium was uniformly distributed on MOF-5 rather than on ZnO, Rh(I)/MOF-5 turned to be a better catalyst. Furthermore, Rh(I)/MOF-5 exhibited excellent recyclability and was reused at least six times without any significance loss in activity.

In the above-described systems, the authors postulated the single-site isolation of the rhodium species as single-atom catalysts, but the formation of small clusters cannot be ruled out, especially under hydroformylation catalytic conditions. The low metal loading reported here, aiming at obtaining high turnover numbers for the hydroformylation reaction, limited the in-depth characterization of the heterogenized rhodium species at the molecular scale, including the rhodium coordination, using standard spectroscopic techniques.

Another methodology for ligand-less rhodium heterogenization within MOFs relied on the encapsulation of Rh nanoparticles.

In 2014, another well-known and highly porous MOF, namely, ZIF-8 (ZIF: zeolitic imidazolate framework) was used as solid support by Li and co-workers for the heterogenization of rhodium.[45] To synthesize Rh@ZIF-8, $RhCl_3$ was infiltrated first in the MOF and then Rh^{3+} was reduced with aqueous $NaBH_4$. PXRD of Rh@ZIF-8 confirmed that the structural integrity was maintained, as well as the absence of additional peaks corresponding to rhodium metal. Moreover, a decrease in BET surface area of 1,366 $m^2\ g^{-1}$ for ZIF-8 to 1,178 $m^2\ g^{-1}$ was reported due to the incorporation of rhodium species. TEM images exhibited finely dispersed homogeneously distributed small rhodium nanoparticles in the Rh@ZIF-8. Authors used this Rh@ZIF-8 catalyst for the hydroformylation reaction of hex-1-ene, hept-1-ene, oct-1-ene, dodec1-ene, tetradec-1-ene, and styrene. In this study also, the major products were found to be linear and branched aldehydes along with isomerized alkenes. An increment in the yield of aldehydes was reported with increasing pressure of syngas ($CO:H_2$) and reached maxima at 5.0 MPa. With prolonged reaction time, the yield of respective aldehydes was increased, while the selectivity (ration between linear and branched aldehydes) was decreased. Again, recyclability of the catalyst was checked and even after five cycles the catalyst was found to be active without any significant loss activity.

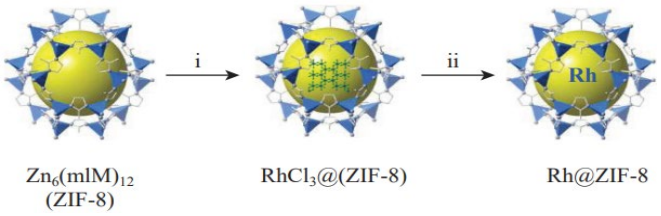

Figure 2. Schematic representation of preparation of $RhCl_3$@ZIF-8 (i) and Rh@ZIF-8 (ii) from ZIF-8. Reproduced with permission from ref. 46. Copyright 2022, Elsevier.

Recently, in another report by Vlasenko *et al.*, ZIF-8 was employed as heterogeneous support for the Rh-nanoparticles for the preparation of solid catalysts.[46] In a stepwise synthesis, $RhCl_3$@ZIF-8 was prepared first by infiltration of $RhCl_3$ and then subsequent reduction with $NaBH_4$ led to the formation of Rh@ZIF-8 (Fig. 2). Both $RhCl_3$@ZIF-8 and Rh@ZIF-8 were used as catalysts for the hydroformylation reaction of styrene and 1-decene. In the case of styrene, only 2% and 12% conversion of styrene were observed for $RhCl_3$@ZIF-8 and Rh@ZIF-8, respectively. Such low conversions were explained in terms of mismatch between the pore sizes of respective catalysts and the size of styrene molecules, which led to the inefficiency of the MOF catalyst. Furthermore, when styrene was replaced by 1-decene as substrate, 89% of conversion was obtained with Rh@ZIF-8 with a ratio of 1325:1 to branched aldehyde over the linear isomer. Again, the leaching test was performed through hot-filtration experiment, where the respective catalyst was filtered off after 1 hour and then the reaction was continued for 24 hours with the filtrate. No increase in the product formation was found indicating that no leaching of the active species occurred during the catalytic process.

Moreover, in 2020, Chen *et al.* demonstrated use of ZIF-8 for the fabrication of Rh-based heterogeneous catalyst in a different approach by preparing core-shell based composite materials.[47] The Rh/ZnO_{50}@ZIF-8 core-shell structure catalyst was prepared in two steps, in first step Rh/ZnO_{50} was synthesized through impregnation of rhodium in ZnO support and in the second step ZIF-8 shell was built around the Rh/ZnO_{50}, where ZnO played the role of sacrificial zinc source for the MOF synthesis. Three different ZnO were used as solid support, namely home-made ZnO_{50}, ZnO-C (commercial ZnO) and ZnO-S (spherical ZnO), for the preparation of Rh/ZnO_{50}, Rh/ZnO-C, and Rh/ZnO-S, respectively. Moreover, in the hydroformylation reaction of dodec-1-ene under 40 MPa of syngas and at 90 °C, the efficiency order (in terms of aldehyde selectivity) was found to be, Rh/ZnO-C> Rh/ZnO-S> Rh/ZnO_{50}. However, in case of Rh/ZnO-C and Rh/ZnO-S, huge leaching of rhodium was observed as compared to Rh/ZnO_{50}. The initial catalytic activity of Rh/ZnO_{50}@ZIF-8 towards hydroformylation of dodec-1-ene was comparatively lower than that of the Rh/ZnO_{50} catalyst, due to the shielding effect of ZIF-8. However, due to the presence of ZIF-8 shell, leaching of Rh during the catalysis was reduced from 18.2% Rh/ZnO_{50} catalyst for to 0.55% for Rh/ZnO_{50}@ZIF-8 after the first catalytic run. And this retention of rhodium species in the core-shell catalyst led to maintaining the catalytic efficiency of the catalyst even after four runs of catalysis showcasing the stability of the catalyst. Moreover, other olefins with shorter chains than dodec-1-ene, *i.e.*, hex-1-ene, oct-1-ene, and dec-1-ene, were used as substrates and a better catalytic efficiency was obtained owing to their smaller sizes.

Furthermore, in 2022, the effect of the pore size and shape of MOFs on the catalytic activity for the hydroformylation reaction was demonstrated by Sun *et al.*, where three Zr-MOFs (namely, UiO-66, UiO-67 and MOF-808) were used as the solid support of Rh-catalysts.[48] Both UiO-66 and UiO-67 had the same *fcu* topology constructed with porous tetrahedral and octahedral cages (Fig. 3). Being made with biphenyl-4,4′-dicarboxylic acid (H_2BPDC), which was bigger than 1, 4-benzenedicarboxylic acid (H_2BDC) linker of UiO-66, UiO-67 was found to have bigger internal pore diameters of 8 Å x 11 Å than UiO-66 (6 Å x 8.4 Å). On the other hand, MOF-808 with *spn*-type topology was synthesized with benzene-1,3,5-tricarboxylic acid (H_3BTC) and consisted of tetrahedral cages and large adamantine unit with pore diameters of 4.8 Å and 18.4 Å, respectively (Fig. 3). All catalysts, namely Rh@UiO-66, Rh@UiO-67, and Rh@MOF-808 were synthesized by infiltration of Rh(acac)(cod) in the respective MOFs. The PXRD patterns of all catalysts showed no major changes compared to as-synthesized MOFs, without any Rh-metal reflections. From TEM studies, highly dispersed nanoparticles were obtained in every cases. Due to the low concentration of rhodium inside the MOFs, metal content could not be detemined through XPS study. Whereas, in case of UiO-systems, significant shifts in the binding energy of oxygen and zirconium were observed as described in earlier examples. This led the authors concluded that rhodium species were located near to zirconium and/or oxygen atoms in the UiO-66 and UiO-67. In contrast, binding energy of zirconium in MOF-808 remained unaffected in Rh@MOF-808. Thereafter, these catalysts were used for the hydroformylation of hex-1-ene, oct-1-ene, dec-1-ene, dodec-1-ene and hexadec-1-ene at 100 °C under 50 bar of syngas (1:1 CO:H_2). Both *n*- and *i*-aldehydes were formed, but no hydrogenation products were obtained. It is noteworthy that neither hydroformylation products nor the isomerization of double bonds in olefins were obtained only with Zr-MOFs without Rh-infiltration. Among the aforementioned olefins, conversion of hex-1-ene was much faster as compared to other olefins. Moreover, the conversion of olefins was faster with Rh@UiO-67 and Rh@MOF-808 catalysts as compared to Rh@UiO-66, which might be attributed to mass transfers limitations in small pore MOF. Again, aldehydes yields were higher in case of Rh@UiO-67 than with Rh@MOF-808. Authors speculated the location of rhodium catalysts in small pore cages for Rh@MOF-808, where tripodal linker positioned at the faces of respective windows of SBU hindered the access of active sites, especially for *i*-alkenes (Fig. 3). Accordingly, the authors sketched out three crucial factors which governed the catalytic activity:

(i) the pore size of the catalysts to allow facile diffusion,

(ii) the location and accessibility of the active rhodium sites in the respective SBUs, and

(iii) the arrangement of substrates (alkenes) inside the confined space of pores.

In the case of the hydroformylation of 1-alkenes, *n*/*i*-aldehydes ratios with all catalysts were found to decrease drastically when duration of the reaction was changed from 5 hours to 21 hours. This was due to the conversion of *i*-alkenes, formed by isomerization, into corresponding *i*-aldehydes.

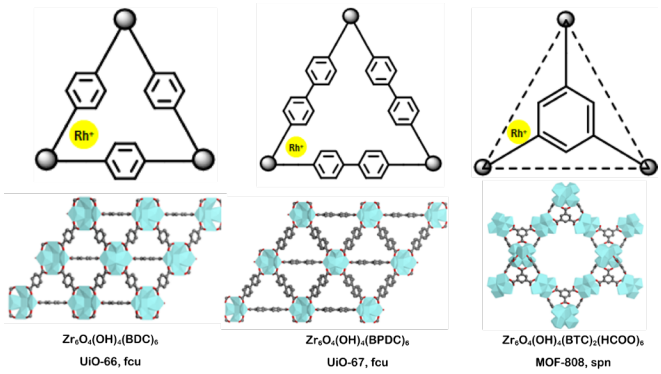

Figure 3. Schematic representation for the structures and topologies of UiO-66, UiO-67 and MOF-808, and probable location of rhodium catalysts inside the respective MOFs. Reproduced with permission from ref. 48. Copyright 2022, Elsevier.

2.2 Cobalt-catalyzed hydroformylation of olefins with MOFs

MOF-based heterogeneous catalysts for hydroformylation reaction are not only limited to the Rh-infiltrated MOFs, recently Co-based molecular catalyst and MOFs were used together. In 2020 Ranocchiari and co-workers reported $Co_2(CO)_8$ catalyst for hydroformylation of olefins along with MOF in the reaction mixture, where micropores of MOFs pushed towards better efficiency, especially for a better selectivity to branched aldehyde.[49] In this regard, authors used various MOFs with different metal nodes and different pore sizes to evaluate the role of microporosity towards the yield and selectivity of aldehydes. MixUMCM-1-NH_2 (UMCM: University of Michigan Crystalline Material) with a molecular formula of $[Zn_4O(btb)_{4/3}(bdc)_x(abdc)_{1-x}]_n$ (btb: 4,4′,4′′,-benzene-1,3,5-triyl-

trisbenzoate, bdc: 1,4-benzenedicarboxylate and abdc: 2-amino-1,4-benzenedicarboxylate) and MOF-74(Zn) with a formula of $[Zn_2(dobdc)]_n$ (dobdc: 2,5-dioxido-1,4-benzenedicarboxylate) showed good conversion of 1-hexene with excellent branched aldehyde selectivity at 100 °C and syngas pressure of 30 bar (Fig. 4a and 4b). At temperature higher than 100 °C a significant amount of isomerization of the respective olefins was reported, whereas at pressure higher than 30 bar lower selectivity to branched aldehydes was obtained. MixUMCM-1-NH_2 (28% of amino-functionalized linker) along with 0.23mol% of Co converted 36% of the olefins with 75% selectivity to branched aldehyde under the aforementioned conditions. After catalysis, it was observed from ICP-MS (Inductively coupled plasma mass spectrometry) that 73% of Co was adsorbed by the MOF. On the other hand, MOF-74(Zn) demonstrated a superior performance with 85% selectivity and 25% conversion of 1-hexene, where 60% of Co-catalyst was adsorbed by the MOF. Again, MOF-74 with Mg, Co and Ni metal nodes were explored for the catalysis to compare with MOF-74(Zn). A low conversion of olefin was observed for MOF-74(Mg) due to small amount of Co-catalyst adsorption during the reaction. However, both MOF-74(Co) and MOF-74(Ni) demonstrated improved conversion of olefin (90% and 44%, respectively), but the selectivity decreased drastically to 55%. Moreover, MIL-101-NH_2(Al), MIL-101(Cr) and Zeolite-Y were also examined under similar conditions with Co-catalyst, but they didn't produce any significant amount of products. To gain more insight regarding the catalytic process and understand the experimental results, authors carried out computational studies. The Monte Carlo simulation exhibited that micropores of the MOFs were able to create the suitable conditions to tune the concentration of corresponding reactants, and thus could push the kinetic limit of the homogeneous reaction favoring the formation of the branched aldehydes. Moreover, as a function of syngas pressure the correlation between branched-to-linear ratio obtained from experimental data and calculated data was shown.

A synergistic effect of the MOF used in addition to Co catalyst was further evidenced for the subsequent Aldol condensation , known as a side reaction of olefins hydroformylation. Very recently in 2023, the same group reported the tandem one pot hydroformylation-Aldol condensation reaction by employing Zn-MOF-74 along with the $Co_2(CO)_8$ for the hydroformylation of 1-hexene followed by the Aldol condensation of the aldehyde to α,β-unsaturated aldehydes under comparatively mild conditions (Fig. 4c).[50] They showed that the cooperative effect of $Co_2(CO)_8$ and Zn-MOF-74 played a crucial role for the enhanced production of the aldol condensation products.

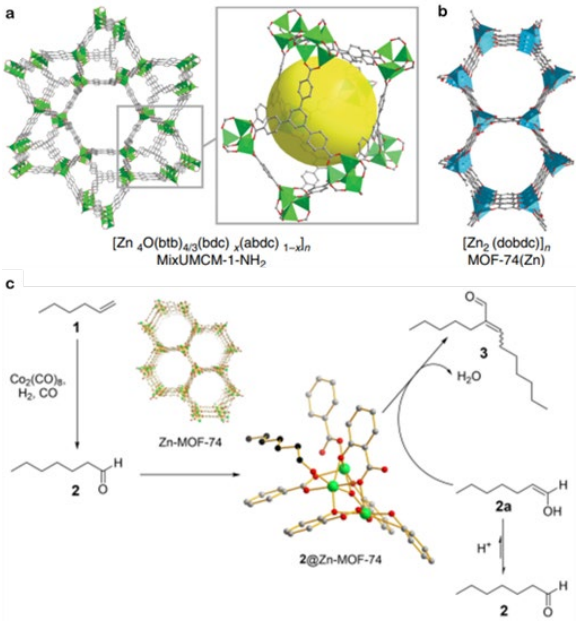

Figure 4. Structures and molecular formulas of a) MixUMCM-1-NH_2 and b) MOF-74 (Zn); c) Proposed reaction mechanism of the tandem hydroformylnation-aldol condensation reaction (Only linear products are included for better clarity. Color code: MOF-74(Zn) carbon (grey), aldehyde carbon (black), oxygen (red), zinc (green), and hydrogen atoms are omitted for clarity. a) and b) Reproduced with permission from ref. 49. Copyright 2020, Nature publishing group. c) Reproduced with permission from ref. 50. Copyright 2023, Wiley-VCH.

2.3 Immobilization of Rhodium/Cobalt-based molecular catalysts in MOFs for hydroformylation of olefins

The following reports deal with the use of molecular rhodium and cobalt complexes where organic ligands in the first coordination sphere of the metal influence the catalytic activity.

In 2015, Sartipi *et al.* demonstrated that polyoxometalate and MOFs can be used in combination for the preparation of Rh-incorporated heterogeneous catalyst for the hydroformylation reaction.[51] Interestingly, this catalyst could act as homogeneous catalyst in presence of CO molecules, since CO molecules are able to form stronger bonds with rhodium molecules by replacing weakly coordinating polyoxometalate. This resulted in the release of active rhodium species in the reaction medium which could act as homogeneous catalyst. However, after the reaction and in the absence of CO, rhodium binds again to the polyoxometalate in a release-and-catch process. In this regard, authors employed porous composite material synthesized of phosphotungstic acid (PTA) and MIL-101(Cr), namely 15PTA-MIL-101(Cr) and 30PTA-MIL-101(Cr) (15 and 30 are the wt% of PTA, respectively). Then, $RhH(CO)(PPh_3)_3$ was infiltrated in 15PTA@MIL-101(Cr) and 30 PTA@MIL-101(Cr) in toluene at 70 °C temperature. Diffuse-reflectance infrared Fourier transform (DRIFT) spectra revealed characteristic vibrational bands corresponding to PTA (1083 cm^{-1} assigned to P-O) and the Rh complex (1119 and 1973 cm^{-1}). Again, ICP-OES analysis confirmed the presence of Rh, where 0.25 and 0.88 wt% of Rh were obtained in Rh-15PTA@MIL-101(Cr) and Rh-30PTA@MIL-101(Cr), respectively. Hydroformylation of oct-1-ene with

homogeneous catalyst $RhH(CO)(PPh_3)_3$ led to 100% conversion after 4 hours, with the formation of isomerized alkenes, nonanal, 1-methyloctanal, and other branched aldehydes. The product selectivity was found to be similar with rhodium infiltrated 15PTA-MIL-101(Cr) and 30PTA-MIL-101(Cr) catalysts. Recovered catalyst was tested again for successive reactions under the same conditions, which revealed that both conversion and selectivity remained unchanged even after six catalytic runs, although the regioselectivity decreased slightly after the first run. When only Rh@MIL-101(Cr) without PTA was employed as catalyst for hydroformylation of oct-1-ene, the conversion reduced from 37% in the first run to 5% in the second run. This result pointed out the role of PTA in this case as an anchoring agent for immobilization of Rh-complex in the PTA-MIL-101(Cr) composite material.

In 2020, Tang *et al.* demonstrated the confinement effect of MOF to achieve chemoselectivity in hydroformylation of styrene.[52] In this report, a manganese-based MOF, namely, MnMOF, with a molecular formula of $[Mn_3(L)_2(L')]$, (where, LH_2: bis (4-(4-carboxyphenyl)-1H-3, 5-dimethylpyrazolyl)methane), and L′ : bis(3,5-dimethylpyrazol-1-yl)methane) was used as the host material to prepare Rh- or Co-based heterogeneous catalysts. Site-isolated rhodium or cobalt molecular catalysts were obtained through chelation to dipyrazole groups inside the MnMOF (Rh/MnMOF and Co/MnMOF, respectively). PXRD patterns of all materials were in accordance with the calculated PXRD patterns of the parent MnMOF, which indicated the absence of nanoparticles or oxidized Rh or Co aggregates. Again, upon metalation the flexibility of the dipyrazole linker in MnMOF was speculated to be hindered, since step at low pressure range in the N_2 adsorption study (at 77 K) for the respective MOF was diminished after chelation of dipyrazole moieties with Rh(I) or Co(II). Moreover, XPS study showed the presence of soft ligated Rh(I) and Co(II) species in the respective MnMOF-based catalysts. Rh/MnMOF showed 100% conversion of styrene with a regioselectivity of 69% at 80 °C and 8 MPa of syngas after 18 hours of reaction. When the reaction was carried out at 50 °C with the same pressure of syngas, almost negligible amount of product was obtained. On the other hand, when the pressure of syngas was reduced to 4 MPa at 80 °C the catalytic performance of Rh/MnMOF was decreased with a 60% conversion of styrene after 18 hours. However, in recycling experiment at 80 °C and 4 MPa, a drastic decrease in conversion of styrene was observed in the next two runs with 18% and 11%, respectively. But recycling with Rh/MnMOF at 80 °C and 8 MPa pressure of syngas showed almost stable activity with slight reduction in the conversion after third cycle, whereas regioselectivity was maintained. In contrast, negligible amount of styrene conversion was obtained with Co/MnMOF at 8 MPa and 80 °C after 18 hours, and same result was found even at 120 °C after 24 hours with a substrate-to-cobalt ratio of 1000:1. When substrate to cobalt was changed to 50:1, 60% conversion of substrate was obtained, but only with partial chemoselectivity. 30% ethylbenzene was observed as a result of hydrogenation with Co/MnMOF along with branched to linear molar ratio of 24:6. Such a reduction in performance from Rh/MnMOF to Co/MnMOF was explained by the leaching test. Rh/MnMOF was found to be a stable catalyst after the reaction, but leaching of both Co and Mn was observed in case of Co/MnMOF. So, lack of stability of the Co/MnMOF led to poorer performance and inability to recycle in hydroformylation of styrene. Rh/MnMOF demonstrated efficient performance towards hydroformylation of styrene with high yield and regioselectivity comparable to that of the homogeneous analogues, which depicted the accessibility of the active sites without any pore blocking effects.

The heterogenization of molecular catalysts based on rhodium and phosphine linkers in MOFs has also attracted much interest in recent years. Very recently, Dong et al. demonstrated three different strategies to immobilize Rh-phosphine based molecular catalyst in MOF-5 (Fig. 5),[53]

(*a*) by impregnating phosphine (PPh_3) linker in rhodium loaded MOF-5 to coordinate the Rh-sites, namely 1Rh-P/MOF-5

(*b*) by incorporating PPh_3 into the pores of MOF-5 during the synthesis at first, and then rhodium was infiltrated to form Rh-PPh_3 molecular catalysts inside MOF material, namely 1Rh/MOF-5-P

(*c*) by infiltrating the rhodium precursor in a modified MOF-5 containing covalently linked phosphines through peptide bonds, namely 1Rh/MOF-5-PPh_3

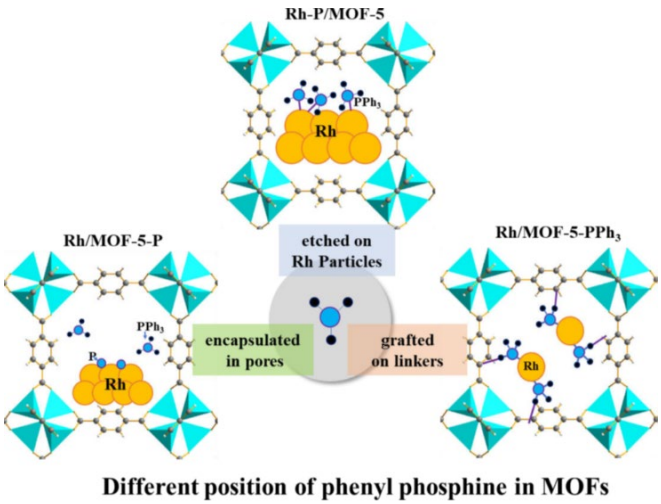

Figure 5. Schematic representation of spatial position of PPh_3 and the effect of linkers on the Rh active sites in MOF-5 prepared three different methodologies. Reproduced with permission from ref. 53. Copyright 2023, Elsevier.

In all cases the structural integrity was maintained, as confirmed by PXRD analysis of all samples. Again, to examine the role of phosphine linkers for the formation of Rh-Phosphine molecular complexes, different amounts of phosphine linkers were infiltrated in each of three different techniques. Different loading of phosphine linkers was assigned as the P/Rh ratio, and the number was mentioned to name the particular catalyst. The coordination between rhodium and the phosphine linkers was investigated through XPS studies. Also, a shift in the binding energy corresponding to rhodium atom was noticed with increasing amount of impregnated PPh_3, and it reached saturation with a P/Rh ratio >8. Moreover, these well characterized catalysts were employed for hydroformylation of 1-butene at 100 °C under 20 bars of syngas (1:1 $CO:H_2$) for 4 hours. For the system of 1Rh-P/MOF-5, it was observed that with increasing amounts of phosphine linkers the activity of the respective catalyst increased. Again, along with the increased activity, yield of aldehyde (pentanal) was improved as well as

the *n/i*-aldehydes selectivity was enhanced from 0.86 for 1Rh/MOF-5 to 1.93 for 1Rh-32P/MOF-5 (where, P/Rh: 32), respectively. Such enhancement in the activity and selectivity with increment in the impregnation of PPh_3 was obtained due to the better stability of the molecular catalyst. On the other hand, catalysts prepared by following the protocol (*b*), namely 1Rh/MOF-5-P, didn't show any significant increment with increasing PPh_3 linkers in MOF-5. Although a small improvement from 0.88 for 1Rh/MOF-5-4P to 0.96 for 1Rh/MOF-5-16P in the *n/i*-aldehydes selectivity was observed at higher P/Rh ratio. Low activity and selectivity for 1Rh/MOF-5-xP was observed due to the low impregnation of PPh_3 leading to less stabilized Rh-PPh_3 catalyst. While, in the case of 1Rh/MOF-5-PPh_3 a reduction in conversion of olefin was observed with increased amount of PPh_3, however, significant improvement in the yield of aldehyde (pentanal) and *n/i*-aldehydes selectivity was observed. The best result was obtained for the 1Rh/MOF-5-32PPh_3 catalyst (where P/Rh: 32). When the homogeneous analogue of this catalyst was tested under the same condition, a slightly higher conversion of 1-butene and yield of aldehyde were found. Also, 1Rh/MOF-5-32PPh_3 showed better *n/i*-aldehydes selectivity as compared to its homogeneous analogue, which was attributed to the confinement effect of MOF-5. Moreover, to investigate the effect of covalently linked and physisorbed phosphine linkers on the catalytic activity, authors compared the results of 1Rh/MOF-5-32PPh_3 and 1Rh-32P/MOF-5, respectively. Although the conversion of alkene was more efficient with 1Rh-32P/MOF-5, aldehyde selectivity (especially, *n/i*) was better with 1Rh/MOF-5-32PPh_3. Again, 1Rh-32P/MOF-5 showed poor result in recycling experiment, where the activity of the catalyst decreased drastically after the third run. Nonetheless, the efficiency of 1Rh/MOF-5-32PPh_3 was maintained even after the sixth catalytic runLeaching test of 1Rh/MOF-5-32PPh_3 catalyst demonstrated no leaching of rhodium. Therefore, this study not only showed the importance of phosphine linkers to stabilize the molecular catalysts for efficient hydroformylation reaction, but also the usefulness of covalent grafting of such linkers inside the porous network of the MOFs.

Very recently another way to immobilize the single-site molecular catalyst in MOF was demonstrated by our group. In contrast to the aforementioned study, here the phosphine linker was not covalently linked to the organic ligand of the MOF; rather it was attached to the metal-node by carboxylate ligand exchange.[54] The 4-diphenylphosphinobenzoic acid (DPPB) was grafted on the $Zr_6O_4(OH)_6$ node of the MOF-808 by linker exchange with native formate (Fig. 6a). Upon successful grafting of phosphine linker inside the pores, rhodium precusors were infiltrated to prepare Rh-phosphine molecular catalysts (Fig. 6a). Solid-state ^{31}P-NMR studies of aforementioned materials demonstrated negligible amount of oxidation of phosphine linker during the synthesis. Two different Rh-precursors were used for the infiltration ($Rh(CO)_2(acac)$ (acac: acetylacetonato) and $RhH(CO)(PPh_3)_3$), and rhodium loading was found to be decreased with the increasing concentration of DPPB linkers in MOF-808. PXRD analysis of all the catalysts showed that structural integrity was maintained even after linker grafting followed by rhodium infiltration. In order to gain more structural details of these catalysts, authors carried out density functional theory (DFT)-level computations. In the case of catalyst obtained from $RhH(CO)(PPh_3)_3$, one of the PPh_3 linkers was replaced by DPPB linker grafted in MOF leading to the formation of $RhH(CO)(PPh)_2$(DPPB) species. And this Rh-molecular catalyst was found to be not only coordinated to the DPPB linker grafted in MOF-808 through direct Rh-P bond but also was stabilized via π-π stacking with other neighboring free grafted DPPB linkers. On the other hand, for the catalyst obtained from $Rh(CO)_2(acac)$, the computational studies demonstrated that the most stable form was a square-planar Rh(CO)(acac)(DPPB) species, where one of the CO molecules was replaced by grafted DPPB linker.

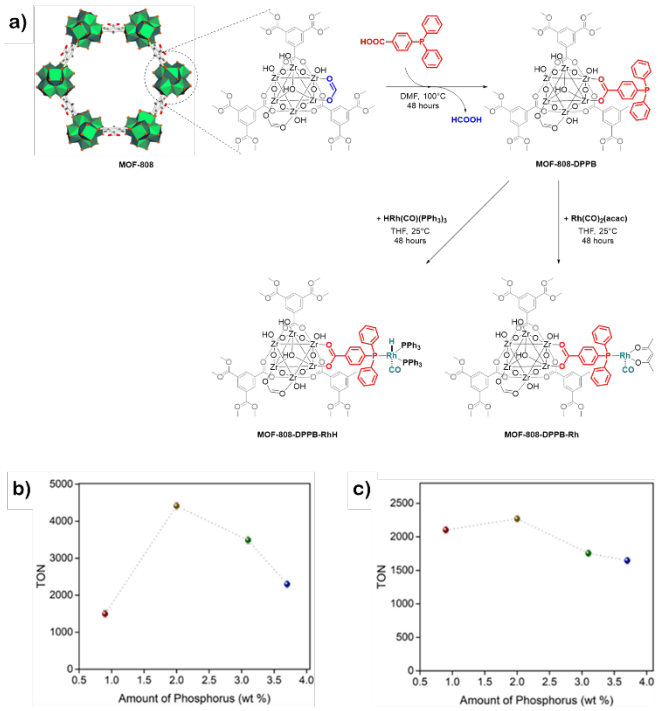

Figure 6. a) Schematic representation for the stepwise synthesis of MOF-808-2.0DPPB-Rh and MOF-808-2.0DPPB-RhH from MOF-808; Catalytic activity of b) MOF-808-2.0DPPB-RhH and c) MOF-808-2.0DPPB-Rh for hydroformylation of ethylene at 110°C temperature and 20 bars pressure of 1:1:1 mixture of C_2H_4:CO:H_2 with time duration of 3 hours. Reproduced with permission from ref. 54. Copyright 2023, American Chemical Society.

Then, all of these catalysts were employed for the hydroformylation of ethylene to propionaldehyde at 110 °C temperature and 20 bars of a 1:1:1 mixture of C_2H_4:CO:H_2 in toluene as solvent. Maximum yield of aldehyde was obtained from the catalysts prepared from 1.3 DPPB linker grafted per Zr-node (i.e., 2.0 wt% of phosphorus) for both rhodium precursors, namely, MOF-808-2.0DPPB-Rh and MOF-808-2.0DPPB-RhH (Fig. 6b and 6c). Furthermore, when the catalysis was performed with MOF-808-2.0DPPB-Rh and MOF-808-2.0DPPB-RhH at varied temperature and pressure, the process was found to be directly proportional to both temperature and pressure. Maximum yield of aldehyde was obtained at 125 °C and 20 bars pressure of gas feed. The MOF-808-2.0DPPB-RhH was found to maintain its efficiency even after the 5th catalytic run without any significant leaching of Rh. The pair distribution function (PDF) analysis of as-synthesized MOF-808-2.0DPPB-Rh and MOF-808-2.0DPPB-RhH showed small difference, however, after catalysis both the catalysts were found to have similar

spectroscopic fingerprints. This result indicated the formation of similar molecular catalysts from the two Rh precusors in MOF-808 after the first cycles of catalysis. This observation was further supported by very similar energy of activation of both catalysts (30 kJ/mol for MOF-808-2.0DPPB-RhH and 32 kJ/mol for MOF-808-2.0DPPB-Rh) obtained from DFT-level calculations. Hence, this study demonstrated the role of linker concentration in catalytic activity, as well as the evolution of the catalysts to their active form during the reaction in well-defined single site molecular catalysts immobilized MOF system.

Summary and Outlook

The growing interest in hybrid porous materials that incorporate organic ligands for molecular complexes has accelerated the development of the heterogenization of molecular catalysts. This heterogenization concept is underpinned by the potential for both the precise control at the molecular level and the advantageous interactions at the solid's interface. While the appeal of easy catalyst separation and catalyst recycling is evident, it is imperative to demonstrate the advantages of employing sophisticated and costly materials for heterogenized molecular catalysts. Comparing these heterogenized catalysts across various catalytic conditions is challenging due to differences in the electronic environment between homogeneous complexes and their solid-embedded counterparts. Additionally, the absence of conclusive evidence regarding the true heterogeneity of catalysts, particularly through tests like hot filtration and recycling at low conversions, hinders a comprehensive understanding of their nature. Site-isolated catalysts, which can be considered at the interface between homogeneous and heterogeneous catalysis, offer an ideal platform for exploring the structure-activity relationships, involving molecular chemistry mechanisms, and requiring computational chemistry as well as advanced spectroscopic techniques. For a complete understanding and accurate comparisons, it is essential to unravel the geometry of the active site using a combination of analytical techniques. While computational chemistry has matured enough to provide insights into molecular mechanisms and predict reactivity in homogeneous catalysis, it is still in its infancy for heterogeneous counterparts. Utilizing a single-site catalyst strategy allows for the implementation of knowledge from homogeneous catalysis while treating the solid support as a traditional ligand. However, in the particular case of alkenes hydroformylation, Lewis acid sites at the MOF node can lead to uncontrolled isomerization, despite some examples where such isomerization is controlled by confinement within the porous network. The MOF confined space has indeed been reported to allow for tuning the selectivity as demonstrated for branched aldehydes. Among heterogenization strategies, the covalent grafting of molecular ligands, like phosphines, has been shown to produce more robust and efficient catalytic species, giving rise to less leaching as compared to physiosorbed species, thus ensuring the reusability of the heterogeneous catalyst. In general, it can be concluded that molecular hydroformylation catalyst heterogenized with MOF scaffold behave mechanistically the same than their homogeneous counterpart, the overall main advantages brought by the MOF support being the site-isolation avoiding deactivation and recycling ability to envision more sustainable catalytic processes.

Moreover, transitioning from homogeneous to heterogeneous phase catalysis aims at the final implementation of heterogenized catalysts in fixed-bed reactors for liquid or gas-phase reactions. However, this often necessitates prior shaping of the solid catalyst, which requires non-trivial strategies that depend on the material and application to avoid critical pressure drops. Consequently, the testing of gas-phase reactions in fixed-bed reactors for MOF-based catalysts is seldom reported. Even with well-defined shaping methodologies for gas-phase applications, the rapid discovery of high-performing MOF catalysts through high-throughput testing remains challenging due to the limitations of most syntheses to the lab-scale. Additionally, macroscopic behavior, especially for shaped bodies, plays a pivotal role in heterogeneous catalysis, relying on the study of mechanisms related to adsorption, diffusion, and kinetics through operando techniques.

In conclusion, the implementation of heterogenized molecular catalysis in actual catalytic processes, such as hydroformylation reaction, along with the exploration of novel synthetic pathways not accessible so far through homogeneous catalysis, relies on a collaborative effort from molecular chemistry, materials science, and heterogeneous catalysis. This concerted approach is instrumental in advancing sustainability and innovation in the field.

Acknowledgements

P.S. and J.C. thank the C123 project that has received funding from the European Union's Horizon 2020 research and innovation program under grant agreement no. 814557 and the ANR project FLIPS (ANR-21-CE07-0028). The authors are also grateful to the IRCELYON scientific services.

Keywords: Metal-organic frameworks • Heterogeneous catalysts • Nanoparticles • Molecular catalysts • Hydroformylation

[1] R. Franke, D. Selent, A. Börner, *Chem. Rev.* **2012**, *112*, 5675.
[2] C. Li, W. Wang, L. Yan, Y. Ding, *Front. Chem. Sci. Eng.* **2018**, *12*, 113.
[3] S. Tao, D. Yang, M. Wang, G. Sun, G. Xiong, W. Gao, Y. Zhang, Y. Pan, *iScience* **2023**, *26*, 106183.
[4] D. P. Zhuchkov, M. V. Nenasheva, M. V. Terenina, Yu. S. Kardasheva, D. N. Gorbunov, E. A. Karakhanov, *Pet. Chem.* **2021**, *61*, 1.
[5] Â. C. B. Neves, M. J. F. Calvete, T. M. V. D. Pinho E Melo, M. M. Pereira, *Eur. J. Org. Chem.* **2012**, *2012*, 6309.
[6] Q. Sun, Z. Dai, X. Liu, N. Sheng, F. Deng, X. Meng, F.-S. Xiao, *J. Am. Chem. Soc.* **2015**, *137*, 5204.
[7] Z. Zhang, Q. Wang, C. Chen, Z. Han, X.-Q. Dong, X. Zhang, *Org. Lett.* **2016**, *18*, 3290.
[8] Homogeneous Catalysis--New Approaches to Catalyst Separation, Recovery, and Recycling, .
[9] S. Hanf, L. Alvarado Rupflin, R. Gläser, S. A. Schunk, *Catalysts* **2020**, *10*, 510.
[10] A. Dhakshinamoorthy, H. Garcia, *Chem. Soc. Rev.* **2012**, *41*, 5262.
[11] B. Liu, Y. Wang, N. Huang, X. Lan, Z. Xie, J. G. Chen, T. Wang, *Chem* **2022**, *8*, 2630.
[12] D. E. De Vos, M. Dams, B. F. Sels, P. A. Jacobs, *Chem. Rev.* **2002**, *102*, 3615.
[13] Q. Sun, Z. Dai, X. Meng, F.-S. Xiao, *Chem. Soc. Rev.* **2015**, *44*, 6018.
[14] D. P. Zhuchkov, M. V. Nenasheva, M. V. Terenina, Yu. S. Kardasheva, D. N. Gorbunov, E. A. Karakhanov, *Pet. Chem.* **2021**, *61*, 1.
[15] P. Verma, Y. Kuwahara, K. Mori, R. Raja, H. Yamashita, *Nanoscale* **2020**, *12*, 11333.

[16] K. Zhao, X. Wang, D. He, H. Wang, B. Qian, F. Shi, *Catal. Sci. Technol.* **2022**, *12*, 4962.
[17] K. Motokura, S. Ding, K. Usui, Y. Kong, *ACS Catal.* **2021**, *11*, 11985.
[18] S. Siangwata, C. Williams, N. Omosun, S. Ngubane, G. S. Smith, *Appl. Catal. Gen.* **2021**, *626*, 118362.
[19] F. M. S. Rodrigues, R. M. B. Carrilho, M. M. Pereira, *Eur. J. Inorg. Chem.* **2021**, *2021*, 2294.
[20] P. W. N. M. van Leeuwen, A. J. Sandee, J. N. H. Reek, P. C. J. Kamer, *J. Mol. Catal. Chem.* **2002**, *182–183*, 107.
[21] A. C. Brezny, C. R. Landis, *Acc. Chem. Res.* **2018**, *51*, 2344.
[22] J. Liang, Z. Liang, R. Zou, Y. Zhao, *Adv. Mater.* **2017**, *29*, 1701139.
[23] L. Chen, Q. Xu, *Matter* **2019**, *1*, 57.
[24] H. Konnerth, B. M. Matsagar, S. S. Chen, M. H. G. Prechtl, F.-K. Shieh, K. C.-W. Wu, *Coord. Chem. Rev.* **2020**, *416*, 213319.
[25] M. S. Alhumaimess, *J. Saudi Chem. Soc.* **2020**, *24*, 461.
[26] Y.-S. Wei, M. Zhang, R. Zou, Q. Xu, *Chem. Rev.* **2020**, *120*, 12089.
[27] V. Pascanu, G. González Miera, A. K. Inge, B. Martín-Matute, *J. Am. Chem. Soc.* **2019**, *141*, 7223.
[28] Y.-S. Kang, Y. Lu, K. Chen, Y. Zhao, P. Wang, W.-Y. Sun, *Coord. Chem. Rev.* **2019**, *378*, 262.
[29] J. Liu, L. Chen, H. Cui, J. Zhang, L. Zhang, C.-Y. Su, *Chem Soc Rev* **2014**, *43*, 6011.
[30] L. Zhu, X.-Q. Liu, H.-L. Jiang, L.-B. Sun, *Chem. Rev.* **2017**, *117*, 8129.
[31] A. Dhakshinamoorthy, M. Opanasenko, J. Čejka, H. Garcia, *Catal. Sci. Technol.* **2013**, *3*, 2509.
[32] A. Ahmad, S. Khan, S. Tariq, R. Luque, F. Verpoort, *Mater. Today* **2022**, *55*, 137.
[33] A. H. Chughtai, N. Ahmad, H. A. Younus, A. Laypkov, F. Verpoort, *Chem. Soc. Rev.* **2015**, *44*, 6804.
[34] C.-D. Wu, M. Zhao, *Adv. Mater.* **2017**, *29*, 1605446.
[35] A. Bavykina, N. Kolobov, I. S. Khan, J. A. Bau, A. Ramirez, J. Gascon, *Chem. Rev.* **2020**, *120*, 8468.
[36] A. Corma, H. García, F. X. Llabrés i Xamena, *Chem. Rev.* **2010**, *110*, 4606.
[37] Y. Wen, J. Zhang, Q. Xu, X.-T. Wu, Q.-L. Zhu, *Coord. Chem. Rev.* **2018**, *376*, 248.
[38] R. Rajapaksha, P. Samanta, E. A. Quadrelli, J. Canivet, *Chem. Soc. Rev.* **2023,** DOI: 10.1039/d3cs00188a.
[39] G. Giannakakis, S. Mitchell, J. Pérez-Ramírez, *Trends Chem.* **2022**, *4*, 264.
[40] A. Wang, J. Li, T. Zhang, *Nat. Rev. Chem.* **2018**, *2*, 65.
[41] T. V. Vu, H. Kosslick, A. Schulz, J. Harloff, E. Paetzold, H. Lund, U. Kragl, M. Schneider, G. Fulda, *Microporous Mesoporous Mater.* **2012**, *154*, 100.
[42] T. Van Vu, H. Kosslick, A. Schulz, J. Harloff, E. Paetzold, J. Radnik, U. Kragl, G. Fulda, C. Janiak, N. D. Tuyen, *Microporous Mesoporous Mater.* **2013**, *177*, 135.
[43] T. Van Vu, H. Kosslick, A. Schulz, J. Harloff, E. Paetzold, M. Schneider, J. Radnik, N. Steinfeldt, G. Fulda, U. Kragl, *Appl. Catal. Gen.* **2013**, *468*, 410.
[44] X. Dong, C. Xin, L. Wang, H. Gong, Y. Chen, *Appl. Catal. Gen.* **2022**, *645*, 118848.
[45] C. Hou, G. Zhao, Y. Ji, Z. Niu, D. Wang, Y. Li, *Nano Res.* **2014**, *7*, 1364.
[46] E. S. Vlasenko, I. A. Nikovskiy, Y. V. Nelyubina, A. A. Korlyukov, V. V. Novikov, *Mendeleev Commun.* **2022**, *32*, 320.
[47] L. Chen, J. Tian, H. Song, Z. Gao, H. Wei, W. Wang, W. Ren, *RSC Adv.* **2020**, *10*, 34381.
[48] Y. Sun, J. Harloff, H. Kosslick, A. Schulz, C. Fischer, S. Bartling, M. Frank, A. Springer, *Mol. Catal.* **2022**, *517*, 112005.
[49] G. Bauer, D. Ongari, D. Tiana, P. Gäumann, T. Rohrbach, G. Pareras, M. Tarik, B. Smit, M. Ranocchiari, *Nat. Commun.* **2020**, *11*, 1059.
[50] P. Gäumann, T. Rohrbach, L. Artiglia, D. Ongari, B. Smit, J. A. Van Bokhoven, M. Ranocchiari, *Chem. – Eur. J.* **2023**, *29*, e202300939.
[51] S. Sartipi, M. J. Valero Romero, E. Rozhko, Z. Que, H. A. Stil, J. de With, F. Kapteijn, J. Gascon, *ChemCatChem* **2015**, *7*, 3243.
[52] P. Tang, S. Paganelli, F. Carraro, M. Blanco, R. Riccò, D. Badocco, P. Pastore, C. J. Doonan, S. Agnoli, *ACS Appl. Mater. Interfaces* **2020**, *12*, 54798−54805.
[53] X. Dong, C. Xin, L. Wang, H. Gong, Y. Chen, *Mol. Catal.* **2023**, *538*, 112973.
[54] P. Samanta, A. Solé-Daura, R. Rajapaksha, F. M. Wisser, F. Meunier, Y. Schuurman, C. Sassoye, C. Mellot-Draznieks, J. Canivet, *ACS Catal.* **2023**, *13*, 4193.